ANL-HEP-PR-04-27
EFI-04-08
FERMILAB-PUB-04/034-T

arXiv:hep-ph/0403224 v2 3 Aug 2004

Dark Matter, Light Stops and Electroweak Baryogenesis

C. Balázs[a], **M. Carena**[b] and **C.E.M. Wagner**[b,c]

[a] *HEP Division, Argonne National Laboratory, 9700 S. Cass Ave., Argonne, IL 60439, USA*
[b] *Fermi National Accelerator Laboratory, P.O. Box 500, Batavia, IL 60510, USA*
[c] *Enrico Fermi Institute, Univ. of Chicago, 5640 Ellis Ave., Chicago, IL 60637, USA*

December 9, 2005

Abstract

We examine the neutralino relic density in the presence of a light top squark, such as the one required for the realization of the electroweak baryogenesis mechanism, within the minimal supersymmetric standard model. We show that there are three clearly distinguishable regions of parameter space, where the relic density is consistent with WMAP and other cosmological data. These regions are characterized by annihilation cross sections mediated by either light Higgs bosons, Z bosons, or by the co-annihilation with the lightest stop. Tevatron collider experiments can test the presence of the light stop in most of the parameter space. In the co-annihilation region, however, the mass difference between the light stop and the lightest neutralino varies between 15 and 30 GeV, presenting an interesting challenge for stop searches at hadron colliders. We present the prospects for direct detection of dark matter, which provides a complementary way of testing this scenario. We also derive the required structure of the high energy soft supersymmetry breaking mass parameters where the neutralino is a dark matter candidate and the stop spectrum is consistent with electroweak baryogenesis and the present bounds on the lightest Higgs mass.

1 Introduction

The questions of dark matter and baryogenesis lie at the interface between particle physics and cosmology. Recently, there has been an improved determination of the allowed range of cold dark matter density from astrophysical and cosmological data. The Wilkinson Microwave Anisotropy Probe (WMAP) [1], in agreement with the Sloan Digital Sky Survey (SDSS) [2], determined the matter and baryon density of the Universe to be $\Omega_m h^2 = 0.135^{+0.008}_{-0.009}$ and $\Omega_b h^2 = 0.0224 \pm 0.0009$, respectively, with $h = 0.71^{+0.04}_{-0.03}$. The difference between the matter and baryonic densities fixes the energy density of the cold dark matter as

$$\Omega_{CDM} h^2 = 0.1126^{+0.0161}_{-0.0181}, \tag{1}$$

at 95% CL. Here Ω_{CDM} is the ratio of the dark matter energy density to the critical density $\rho_c = 3H_0^2/(8\pi G_N)$, where $H_0 = h \times 100\ km/s/Mpc$ is the present value of the Hubble constant, and G_N is Newton's constant. Such a precise range of values poses important restrictions to any model of physics beyond the Standard Model (SM) which intends to provide an explanation to the origin of dark matter.

Understanding what the observed dark matter in the Universe is made of is one of the most important challenges of both particle and astroparticle physics, and collider experiments are an essential tool towards solving the dark matter puzzle. Although there are many scenarios to explain the origin of dark matter, weakly interacting massive particles (WIMPs), with masses and interaction cross sections characterized by the weak scale, provide the most compelling alternative. These neutral, and stable particles appear naturally in low energy supersymmetry models, in the presence of R-parity [3]. In a way, dark matter by itself provides a fundamental motivation for new physics at the electroweak scale. Low energy supersymmetry provides an excellent solution to the origin of dark matter and it has been extensively studied in the literature in different scenarios of supersymmetry breaking [4, 5, 6, 7, 8, 9, 10].

In contrast, the origin of the matter-antimatter asymmetry is more uncertain. The three Sakharov requirements [11] for a dynamical origin of the baryon asymmetry may be easily fulfilled in scenarios associated with the decay of heavy, weakly interacting particles. Leptogenesis [12] is an ingenious mechanism that explains the baryon asymmetry as induced from a primordial lepton asymmetry which transforms into a baryon asymmetry through weak anomalous processes. This is a very attractive scenario which yields a connection between baryon asymmetry and neutrino physics. The heavy decaying particle may be identified with the lightest right-handed component of the observable left-handed neutrinos.

One of the drawbacks of scenarios of baryogenesis associated with heavy decaying particles is that they are difficult to test experimentally. The minimal leptogenesis scenario is consistent with the see-saw mechanism for the generation of the small neutrino masses with all light neutrino masses below 0.1 eV [13], but little more can be said without making additional model-dependent assumptions. In particular, the CP-violating phase associated with neutrino oscillations is only indirectly related to the phases associated with the generation of the primordial lepton asymmetry.

Electroweak baryogenesis [14], on the other hand, provides a scenario that relies only on weak scale physics, and therefore potentially testable at present and near-future experiments. Perhaps the most attractive feature of this mechanism is that it relies on anomalous baryon number violation processes which are present in the Standard Model [15]. At temperatures far above the electroweak phase transition critical temperature, these anomalous processes are unsuppressed and, in the absence of any $B-L$ asymmetry, they lead to the erasure of any baryon or lepton number generated at high energy scales [16]. These baryon number violation processes are, instead, exponentially suppressed in the electroweak symmetry broken phase, at temperatures below the electroweak phase transition [17, 18]. The mechanism of electroweak baryogenesis may become effective if the baryon number violation processes in the broken phase are sufficiently suppressed at the electroweak phase transition temperature. This, in turn, demands a strongly first order electroweak phase transition,

$$v(T_c)/T_c \gtrsim 1, \tag{2}$$

where $v(T_c)$ denotes the Higgs vacuum expectation value at the critical temperature T_c.

The strength of the first order phase transition may be determined by studying the Higgs effective potential at high temperatures. The Higgs vacuum expectation value at the critical temperature is inversely proportional to the Higgs quartic coupling, directly related to the Higgs mass squared. For sufficiently light Higgs bosons, a first order phase transition may take place, induced by loop-effects of light bosonic particles, with masses of order of the weak scale, and strong couplings to the Higgs field. The only such particles in the SM are the weak gauge bosons and their couplings are not strong enough to induce a first-order phase transition for any value of the Higgs mass [19].

The condition of preservation of the baryon asymmetry may be easily fulfilled by going beyond the SM framework. Within the minimal supersymmetric Standard Model (MSSM), a first order phase transition is still induced at the loop-level. The relevant bosons are the supersymmetric partners of the top quarks (stops), which couple strongly to the Higgs field, with a coupling equal to the top-quark Yukawa coupling. In addition, a light stop has six degrees of freedom, three of color and two of charge, enhancing the effects

on the Higgs potential. Detailed calculations show that for the mechanism of baryogenesis to work, the lightest stop mass must be smaller than the top quark mass and heavier than about 120 GeV. Simultaneously, the Higgs boson involved in the electroweak symmetry breaking mechanism must be lighter than 120 GeV [20]–[27].

A light stop is an interesting possibility, independently of the question of electroweak baryogenesis. These states were and are being searched for at LEP and the Tevatron collider in various decay modes. The Tevatron reach for a light stop depends on the nature of the supersymmetry breaking scenario, which determines the decay properties of the lightest stop, and also on the specific values of the light chargino and neutralino masses [28, 29, 30, 31, 32]. In this work, we focus on the case in which the lightest neutralino is stable, and provides a good dark matter candidate. In such case, the Tevatron can find a light stop provided its mass is smaller than about 200 GeV [33], a region that overlaps maximally with the interesting one for electroweak baryogenesis.

Within the MSSM, the lightest Higgs boson mass is bounded to be below about 135 GeV [34]. This bound depends crucially on the top spectrum and also on the value of the CP-odd Higgs boson mass, m_A, and the ratio of the Higgs vacuum expectation values, $\tan\beta$. Lighter stops, or values of $\tan\beta$ of order one would push this bound to values closer to the present experimental bound,

$$m_h \gtrsim 114.4 \text{ GeV}, \tag{3}$$

which is valid for a Higgs boson with SM-like couplings to the weak gauge bosons [35]. Consistency of the present Higgs boson bounds with a light stop demands $\tan\beta$ to be large, $\tan\beta \gtrsim 5$, and the heaviest stop to have masses of order 1 TeV or larger. In particular, the requirement of a light Higgs boson, with mass smaller than 120 GeV, necessary for the realization of electroweak baryogenesis, is naturally fulfilled within the MSSM with one stop lighter than the top-quark.

2 Light stop and dark matter constraints

The requirement that the lightest supersymmetric particle provides the observed dark matter of the Universe demands that it should be lighter than the light stop. Assuming that the lightest supersymmetric particle is the superpartner of the neutral gauge or Higgs bosons, namely a neutralino, imposes strong constraints on the values of the gaugino and Higgsino mass parameters. For simplicity, within this work we shall assume that the gaugino mass parameters are related by the standard unification relations, which translate at low energies to $M_2 \simeq 2\, M_1$, where M_2 and M_1 are the supersymmetry breaking masses of the weak and hypercharge gauginos respectively.

Interestingly enough, electroweak baryogenesis demands not only a light stop and a light Higgs boson, but light charginos or neutralinos as well [36]. In particular, values of the Higgsino mass parameter $|\mu|$ and M_2 of the same order, and smaller than about 300 GeV are required. The presence of a light stop, as required for electroweak baryogenesis, and a consistency with the observed relic density of the Universe imposes then interesting constraints on the parameter space.

The introduction of non-vanishing phases is required to fully address the parameter space consistent with electroweak baryogenesis. The required values of the phases in the chargino sector vary in a wide range, $1 \gtrsim \sin\phi_\mu \gtrsim 0.05$, where ϕ_μ is the relative phase between the gaugino and the Higgsino mass parameters [36]. Larger values of this phase are preferred for larger values of the chargino masses and of the CP-odd Higgs mass [36]. Due to the uncertainties involved in the determination of the baryon asymmetries, however, one cannot exclude phases an order of magnitude smaller than the ones quoted above.

Recently, there have been several studies of the effects on the neutralino relic density associated with CP-violating phases in the soft supersymmetry breaking parameters [37, 38, 39]. For large values of the CP-violating phases, these effects are of special relevance in the neutralino annihilation cross section via s-channel Higgs bosons, as well as on direct dark matter detection, due to the CP-violating effects on the couplings and the CP-composition of the Higgs boson mass eigenstates [40]. In general, however, similar effects to the ones coming from CP-violating phases may be induced by changes in the value of the soft supersymmetry breaking parameters in the CP-conserving case.

In this article we limit our study to the case of vanishing CP-violating phases. We expect the CP-conserving case to represent well the constraints that exist for the lower end of values of the phases consistent with electroweak baryogenesis. Moreover, the CP-conserving case addresses the general question about the constraints coming from requiring an acceptable neutralino relic density in the presence of a light stop, like the one accessible at the Tevatron collider. As we shall show, there are relevant implications for stop searches at hadron colliders in general and at the Tevatron in particular, in the region in which the stop co-annihilates with the lightest neutralino. In this region, assuming universal gaugino masses at the GUT scale, the lightest neutralino becomes mainly bino and the resulting annihilation cross section becomes weakly dependent on the CP-violating phases. A detailed study of the CP-violating case demands a calculation that includes non-vanishing phases in a self-consistent way. Work in this direction is in progress [41].

In order to define our analysis, we assume that all squarks other than the lightest stop are heavy, with masses of order 1 TeV, and study the constraints that arise in the μ–

M_1 plane from the requirement of consistency with current experimental bounds and an acceptable dark matter density. Since the change of the sign of μ produces little variation in the selected regions of parameter space, we shall show our results only for positive values of μ. We present results for $\tan\beta = 10$ and 50. Let us stress that the CP-violating sources for the generation of baryon number tend to be suppressed for large values $\tan\beta$, and that values of $\tan\beta$ not much larger than 10 are preferred from those considerations [36]. For $\tan\beta = 10$, we set the first and second generation slepton masses to 250 GeV, to accommodate the measured muon anomalous magnetic moment within one standard deviation[1]. No significant variation of the neutralino relic density is obtained by taking the sleptons to be as heavy as the squarks.

The mechanism of electroweak baryogenesis and the present bounds on the lightest CP-even Higgs mass demand one light-stop and one heavy-stop in the spectrum. Consistency with precision electroweak data is easily achieved by demanding that the light stop is mainly right-handed. The required right- and left-handed stop supersymmetry breaking parameters are $m_{\tilde{U}_3} \simeq 0$ and $m_{\tilde{Q}_3} \gtrsim 1$ TeV, respectively [24]. A non-negligible value of A_t is necessary in order to avoid the Higgs mass constraints. On the other hand, large values of A_t tend to suppress the strength of the first order phase transition. Quite generally, acceptable values of the Higgs mass and of the phase transition strength are obtained for $0.3 \lesssim |X_t|/m_{\tilde{Q}_3} \lesssim 0.5$.

Our choices of the fixed weak scale soft supersymmetry breaking parameters can be summarized as follows

$$\begin{aligned} &m_{\tilde{U}_3} = 0, \quad m_{\tilde{Q}_3} = 1.5 \text{ TeV}, \quad X_t = \mu/\tan\beta - A_t = 0.7 \text{ TeV}, \\ &m_{\tilde{L}_3} \approx m_{\tilde{E}_3} \approx m_{\tilde{D}_3} \approx 1 \text{ TeV}, \quad m_{\tilde{Q}_{1,2}} \approx m_{\tilde{U}_{1,2}} \approx m_{\tilde{D}_{1,2}} \approx 1.2 \text{ TeV}, \\ &M_2 = M_1 g_1^2/g_2^2, \quad M_3 \approx 1 \text{ TeV}. \end{aligned} \tag{4}$$

Computations of masses and couplings at the one-loop level are performed numerically using ISAJET 7.69 [50], to which we input the weak scale soft parameters, listed in Eq.(4) and in the figure captions. To compute the neutralino relic density, we used ISAReD, the computer code which was presented in Ref. [51]. This code agrees well with the public code MicrOmegas [52]. The neutralino-nucleon spin-independent scattering cross sections are computed by the method described in Ref. [53].

Figure 1 shows the regions of parameter space, in the μ–M_1 plane, for which a consistent relic density develops in the presence of a light stop and $\tan\beta = 10$. As we will

[1]The latest calculations show a difference between the experimental [42] and SM central values of the muon anomalous magnetic moment that varies in the range of about 5 and 25 $\times 10^{-10}$ with slight preference toward the higher end [43, 44, 45, 46, 47, 48]. The SUSY contributions to $(g-2)_\mu$ were evaluated using the code described in Ref. [49].

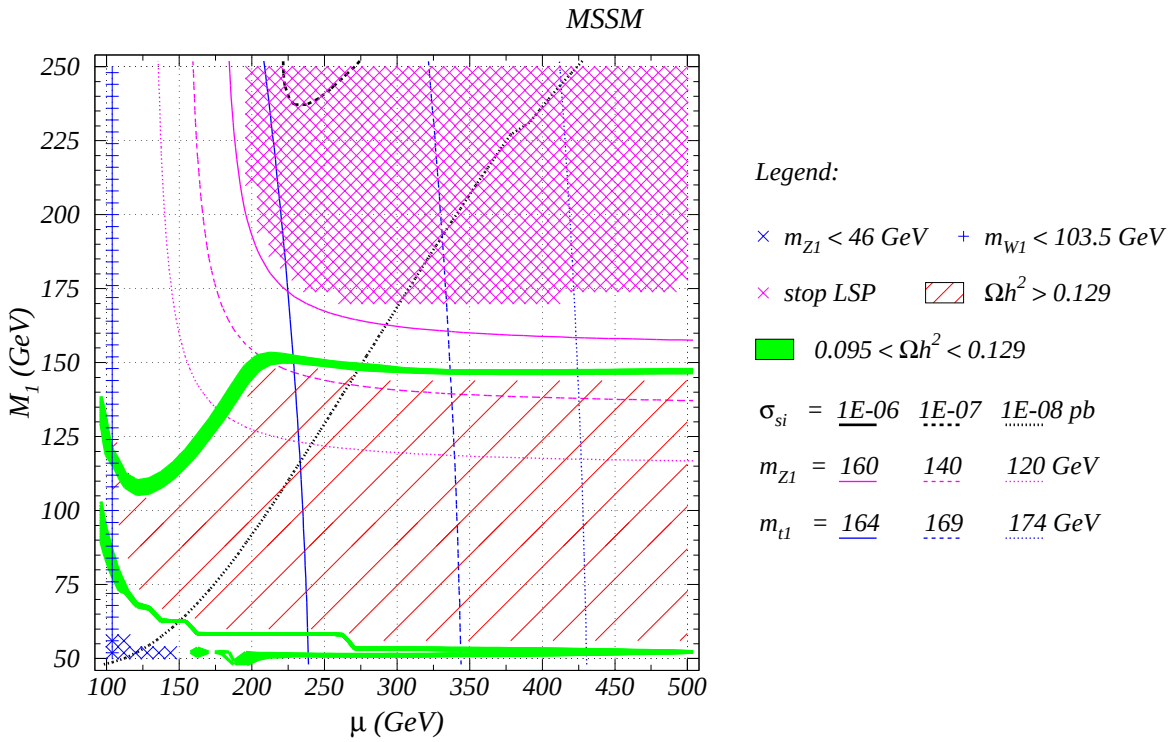

Figure 1: Regions in the μ–M_1 parameter space at which an acceptable value of cold dark matter develops. The green bands show the region where the neutralino relic density is consistent with the WMAP data. The black contours indicate cross section values for neutralino-proton scattering. Neutralino and stop mass contours are also shown. Here we set $\tan\beta = 10$, $m_{\tilde{L}_2} = m_{\tilde{E}_2} = 250$ GeV, and the CP-odd Higgs mass has been chosen to be equal to 500 GeV.

show, the allowed parameter space depends on the value of the CP-odd Higgs mass. In Figure 1, the CP-odd Higgs boson mass was chosen to be 500 GeV and the resulting lightest CP-even Higgs mass lies in the range 115–116 GeV. The solid green (gray) area shows the region of parameter space where a neutralino relic density arises which is consistent with the WMAP observations at the 95% CL. The hatched regions are either incompatible with the neutralino being the LSP (the neutralino becomes heavier than the stop) or excluded by LEP data [54]. The regions of parameter space where the dark matter density is above the experimental upper bound and excluded by more than two standard deviations, are represented by the shaded region in this figure. The white regions are those where the neutralino relic density is below the experimental lower bound. An additional source of dark matter, unrelated to the neutralino relic density, would be necessary in those regions. Constant stop and neutralino mass contours are also shown by solid, dashed and dot-dashed curves, and are given by approximate vertical and hyperbolic lines, respectively.

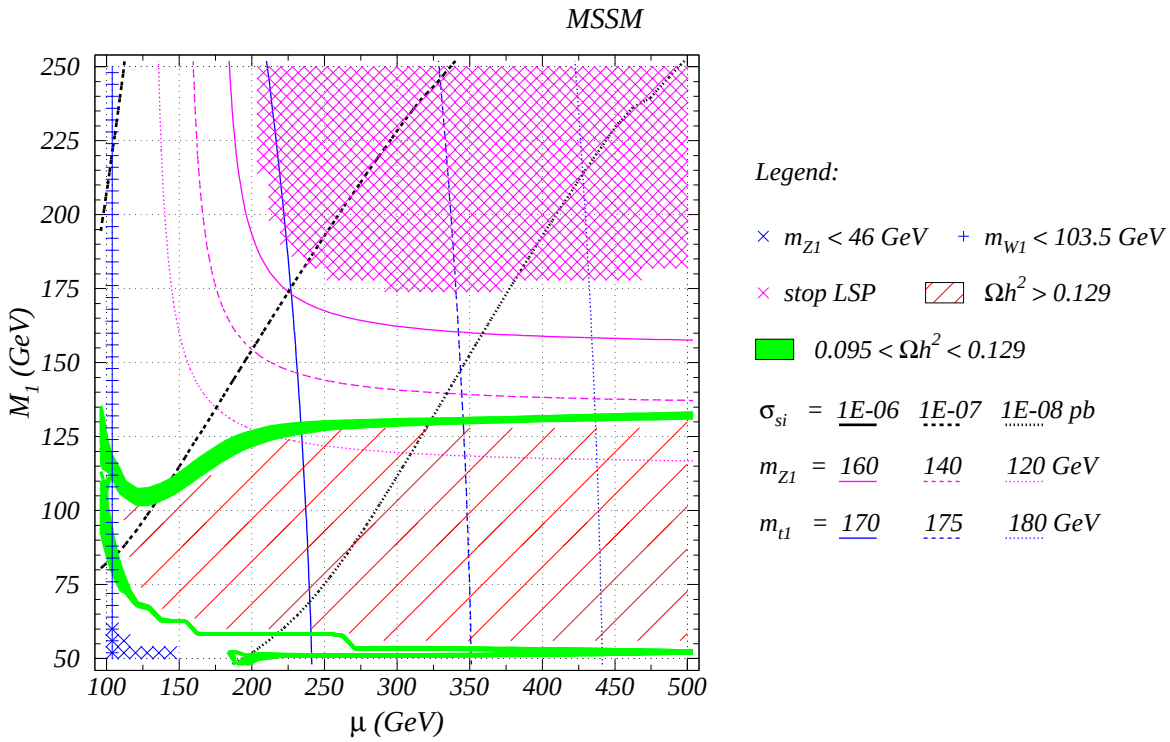

Figure 2: Same as Figure 1, except the CP-odd Higgs mass has been chosen to be equal to 300 GeV.

In Figure 1, there are three qualitatively different regions in which an acceptable relic density arises. First, there is a region of parameter space where the mass difference between the lightest neutralino and the light stop is small. In this region, $M_1 \simeq 150$ GeV, $|\mu| \gtrsim 200$ GeV, stop-neutralino co-annihilation dominates the neutralino annihilation cross section. The stop-neutralino mass difference varies between 20 and 30 GeV in that region, and, as we shall discuss below, presents a challenge for stop searches at hadron colliders.

The second region of parameter space is the narrow band present at small values of M_1 that becomes narrower at large values of μ. This region is associated with the s-channel annihilation of the lightest neutralino via the lightest CP-even Higgs boson. For large values of $|\mu|$ the value of M_1 at which this narrow band develops is approximately given by $M_1 \simeq m_h/2$.

The small width of the band at large values of μ may be explained by the fact that the Higgs-mediated annihilation cross section is proportional to the square of the small bottom Yukawa coupling. Indeed, for $m_A \gtrsim 200$ GeV and large values of $\tan\beta$, the lightest Higgs boson has standard model like couplings to all standard model fermions. The cross section is also proportional to the square of the Higgs-neutralino coupling. This coupling is proportional to both the gaugino and the Higgsino components of the lightest neutralino.

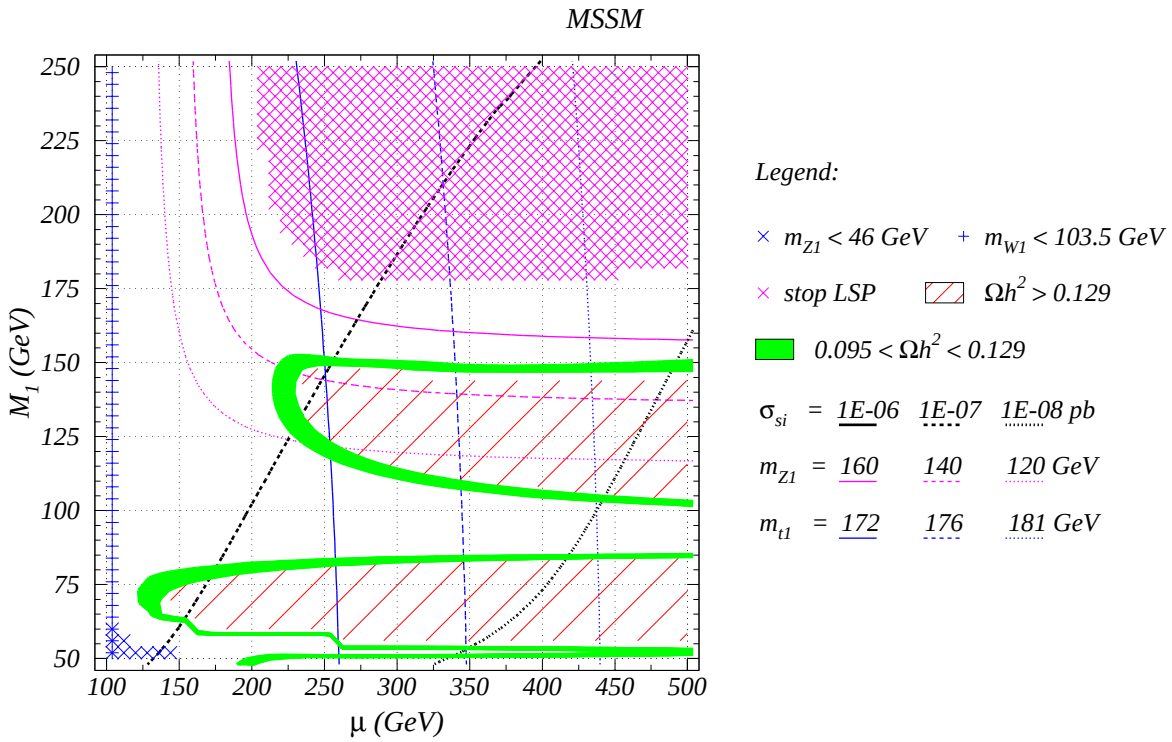

Figure 3: Same as Figure 1, except the CP-odd Higgs mass has been chosen to be equal to 200 GeV.

While for small values of μ the neutralino may annihilate via Z-boson mediated processes, no such annihilation contribution exists for large values of $|\mu|$. Therefore, for large values of $|\mu|$, the Higgs mediated s-channel annihilation proceeds with a strength proportional to the square of the Higgsino component, which decreases for large values of $|\mu|$, and inversely proportional to the square of its mass difference with the Higgs boson. That explains why the band becomes narrower for larger values of $|\mu|$, for which a larger fine tuning between the Higgs and the neutralino masses is necessary in order to produce the desired annihilation cross section. Finally, there is a region for small values of $|\mu|$ and M_1 for which the annihilation receives also contributions from Z-boson exchange diagrams, which become rapidly dominant as the neutralino mass is far from the stop mass or $m_h/2$.

In Figure 1, we also indicate cross section values for spin independent neutralino-proton scattering (σ_{si}). Thick, black contour lines are plotted for $\sigma_{si} = 10^{-7}$ pb (dashed) and $\sigma_{si} = 10^{-8}$ pb (dotted). For the parameters of Figure 1, these direct detection cross section values are close to 10^{-8} pb in the whole displayed region, with the exception of the low μ and high M_1 region, where $\sigma_{si} \sim 10^{-7}$ pb. These cross sections are quite encouraging, since projections of GENIUS, XENON and ZEPLIN indicate future sensitivity even below $\sigma_{si} \sim 10^{-9}$ pb for the neutralino masses of interest [55]. As shown in the subsequent

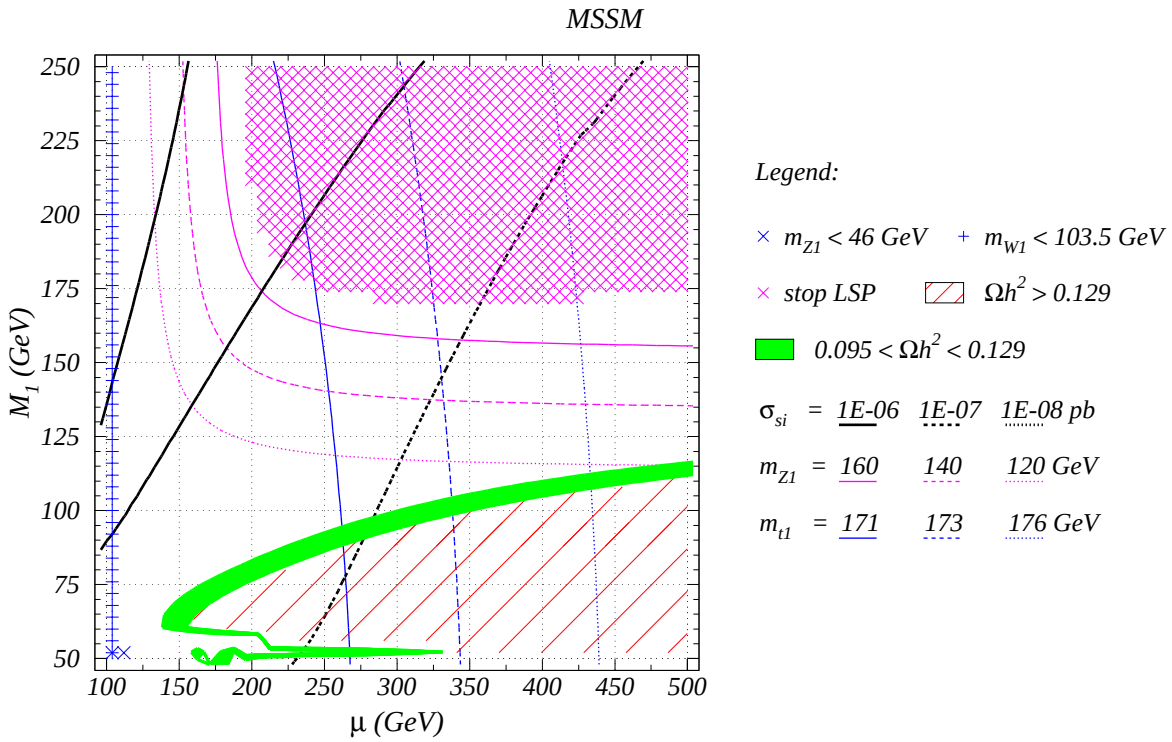

Figure 4: Same as Figure 2, except for $\tan\beta = 50$ and $m_{\tilde{L}_2} = m_{\tilde{E}_2} = 1.1$ TeV.

figures, for lower values of m_A and/or higher values of $\tan\beta$, direct detection cross sections occur up to $\sigma_{si} \sim 10^{-6}$ pb in the examined parameter region. These cross sections are at the reach of several experiments, such as CDMS, EDELWEISS and ZEPLIN. According to their projections, these experiments will reach a sensitivity of a few times 10^{-8} pb, in the next few years [56].

So far, we have kept the CP-odd Higgs mass large, so that the CP-odd Higgs has no impact on the annihilation cross section. Figure 2 shows the case when the CP-odd Higgs mass is lowered to 300 GeV. For this mass value, the CP-odd Higgs and the heavy CP-even Higgs boson contribute to the annihilation cross section in the s-channel resonant region for values of the neutralino mass which are close to the stop mass. Due to the existence of these two annihilation channels for similar values of the neutralino mass, the main effect of this smaller CP-odd Higgs mass is to move the region compatible with the observed relic density slightly away from the stop-neutralino co-annihilation region to lower M_1 values.

In order to better visualize the importance of the CP-odd Higgs mass affecting the stop-neutralino mass difference in the region where co-annihilation is active, in Figure 3 we have plotted what happens when the CP-odd Higgs mass is moved towards even smaller values, of order 200 GeV. In this case, the regions where resonant annihilation via the CP-

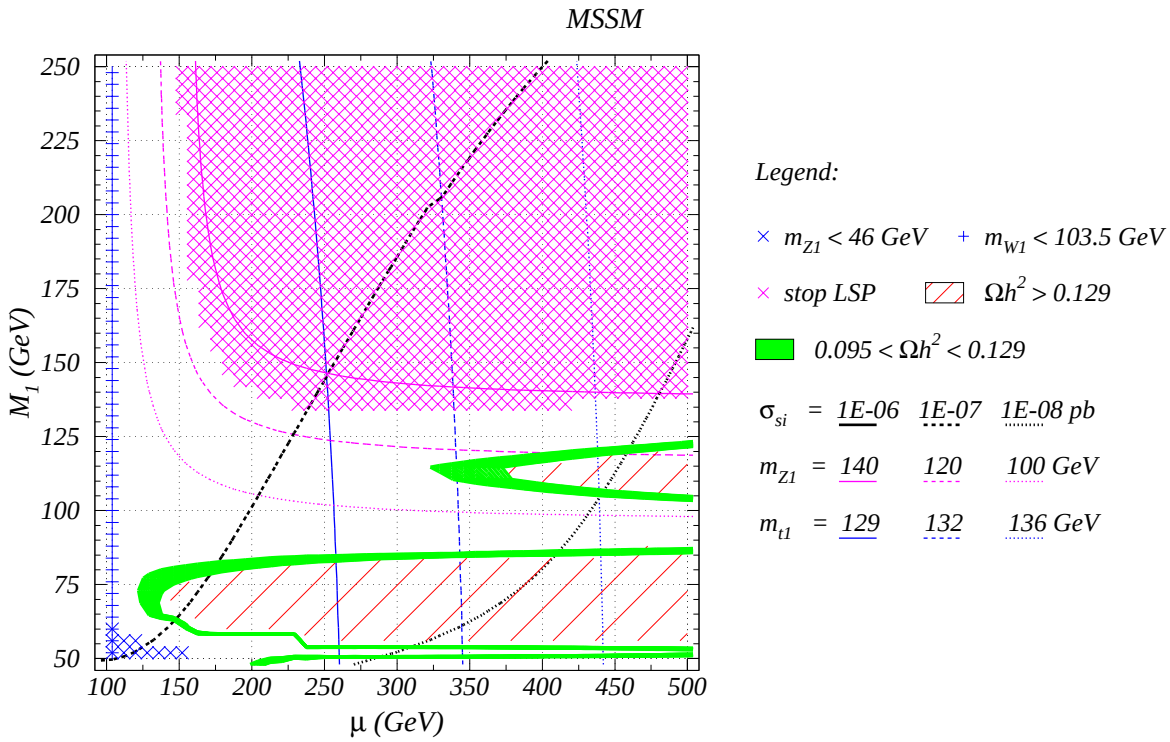

Figure 5: Same as Figure 3, except for $m_{\tilde{U}_3} = -(35\text{ GeV})^2$ and $m_{\tilde{Q}_3} = 1.25$ TeV.

odd and heavy CP-even Higgs bosons takes place are clearly shown. There are now two bands of neutralino masses consistent with dark matter density constraints, that appear at M_1 values of order 100 and 60 GeV, respectively, and that are associated with s-channel annihilation via the lightest and heaviest Higgs bosons, respectively. Observe that the width of the band associated with s-channel annihilation via the CP-odd and heavy CP-even Higgs bosons becomes significantly larger than the ones appearing in Figure 2. This larger region is associated with the $\tan\beta$ enhanced couplings of these particles to bottom quarks and tau leptons, compared to the lightest CP-even Higgs boson. In Figure 3, the stop-neutralino co-annihilation region, which had been modified in Figure 2 due to the presence of the 300 GeV Higgs bosons, recovers the shape presented in Figure 1, with stop-neutralino mass differences of order 20-30 GeV.

Let us comment on the impact of varying the value of $\tan\beta$. The main effect is to change the coupling of the CP-odd Higgs boson and of the heavy CP-even Higgs boson to bottom quarks. This coupling grows linearly with $\tan\beta$ and therefore the annihilation cross section grows quadratically with $\tan\beta$. The growth of the s-channel annihilation cross section has dramatic consequences on the allowed parameter space only if the CP-odd Higgs boson is light. Figure 4 shows the impact of taking $\tan\beta = 50$ for the CP-odd Higgs boson mass equal to 300 GeV. While for $m_A = 500$ GeV, we obtain that there is

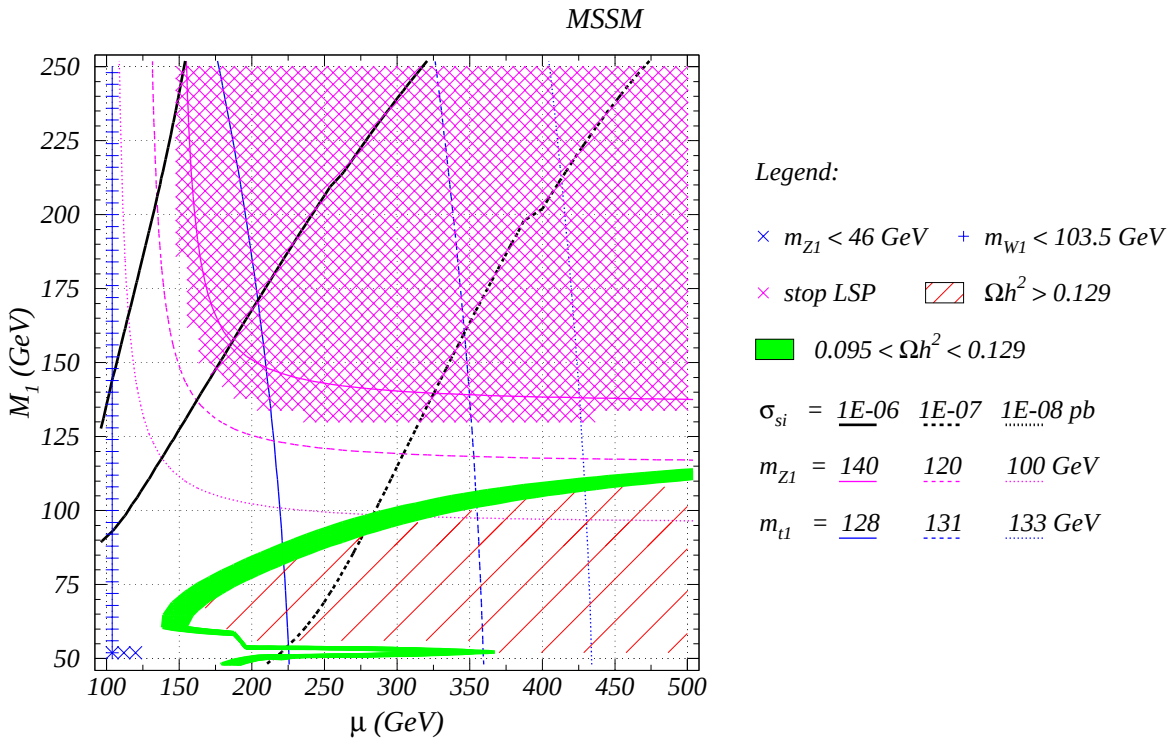

Figure 6: Same as Figure 2, except for $\tan\beta = 50$, $m^2_{\tilde{U}_3} = -(35\ \text{GeV})^2$ and $m_{\tilde{Q}_3} = 1.25$ TeV.

only a small variation with respect to the results of Figure 1, we show in Figure 4 that for $m_A = 300$ GeV the stop-neutralino mass gap becomes larger than the one observed in Figure 2. Finally, for $\tan\beta = 50$ and $m_A = 200$ GeV, we obtain that the effect is sufficiently strong as to make the relic density smaller than the observable one for most of the parameter space. In Figure 4, and for the computations with $\tan\beta = 50$, we have chosen heavy sleptons, to accommodate to the observed values of the muon anomalous magnetic moment.

To further scrutinize the parameter region favorable for baryogenesis, we assigned a small negative value to the square of the right handed stop mass while simultaneously decreasing slightly the left handed doublet mass. The results of the parameter scan are qualitatively the same as the ones presented in Figures 1-4. Figure 5 shows a representative case with $\tan\beta = 10$ and $m_A = 200$ GeV. Due to somewhat lower $\tilde{t}_1$ masses (in the region of 130 GeV) the co-annihilation region is squeezed to lower neutralino mass values. The Higgs annihilation funnels are just the same as in Figure 3. In contrast with the earlier results, the mass gap between the lightest stop and neutralino decreases to about 15 GeV.

Finally, Figure 6 shows a part of the parameter space with negative $m^2_{\tilde{U}_3}$ for $\tan\beta = 50$. For this value of m_A (=300 GeV) the co-annihilation and annihilation regions fuse just

as in Figure 2, but in the co-annihilation region the $\tilde{t}_1$-$\tilde{Z}_1$ mass gap remains about 15-20 GeV. From this exercise of lowering the lightest stop mass, we draw the conclusion that for decreasing stop masses the stop-neutralino mass gap, which is necessary to satisfy the dark matter constraints with co-annihilation, also decreases. Although in this parameter region its mass is well within reach, with the smaller mass gap it is even more challenging for the Tevatron to discover the lightest stop. On the other hand, the direct detection of relic neutralinos remains promising throughout this whole region.

In our analysis, we have not considered the constraints coming from the rare decay of $b \to s\gamma$. In the absence of flavor violating couplings of the down squarks to gluinos this decay imposes a strong constraint on the Higgs and stop spectrum, in particular for large values of $\tan\beta$ [57]. However, this constraint can be avoided in the presence of nontrivial down squark flavor mixing [58, 59]. For instance, assuming all down squark masses are of the order of 1 TeV, even a small left-right mixing of order of $10^{-2} \times m_{\tilde{b}}^2$ between the second and third generation down squarks can induce important corrections to the amplitude of this decay rate, that may compete with the one induced by the Higgs and the stop sectors. This small mixing effects should have only a very small impact on our analysis of the high energy soft supersymmetry breaking parameters.

3 Searches for a light stop at hadron colliders

The search for a light stop in the MSSM depends both on the nature of the supersymmetry breaking mechanism as well as on the mass difference between the light stop and the lightest chargino and neutralino. When the mass difference between the stop and the neutralino is small, the dominant decay channel is a loop induced, flavor violating decay of the stop particle into a charm and the lightest neutralino.

In models with a light stop and the neutralino providing the observable dark matter, the neutralino signature will be associated with missing energy ($\not{E}_T$). Detection of a decaying stop, that has a small mass difference with a lighter neutralino, will depend on the ability of triggering on the missing energy signature. Present Tevatron search simulations for the region in which the two-body charm-neutralino decay is the dominant one are shown in Figure 7 [33]. For 2–4 fb^{-1} of integrated luminosity and neutralino masses smaller than 100 GeV, stops with masses up to about 180 GeV may be detectable under the assumption that the stop-neutralino mass difference is at least 30 GeV. Even larger stop-neutralino mass differences are required for neutralino masses above 100 GeV, and stop detection becomes impossible for neutralino masses above 120 GeV. (Some Tevatron limits are not shown in Figure 7, since they are only effective for neutralino masses below

50 GeV [29].)

In order to examine the stop-neutralino mass gap in the MSSM parameter space favorable for baryogenesis, we conducted a random scan over the following range of supersymmetric parameters:

$$-(20\ \text{GeV})^2 < m^2_{\tilde{U}_3} < 0, \quad 100\ \text{GeV} < \mu < 500\ \text{GeV}, \quad 50\ \text{GeV} < M_1 < 175\ \text{GeV},$$
$$200\ \text{GeV} < m_A < 500\ \text{GeV}, \quad 10 < \tan\beta < 50. \tag{5}$$

The rest of the parameters, which are not scanned, are fixed according to Eq. (4). The result of the scan, projected on the stop mass vs. neutralino mass plane, is shown by Figure 7. The (magenta $\times$) cross hatched area in the upper left corner is excluded since there the stop is lighter than the neutralino. Similarly, the (blue $+$) cross hatched region with stop masses below 95 GeV shows the 95% C.L. exclusion limit of LEP [28]. The green (dark gray) and yellow (light gray) dots represent models in which the relic density is consistent with or below the 2 σ WMAP bounds. (All these models also pass the $m_h > 114.4$ GeV and $m_{\tilde{W}_1} > 103.5$ GeV mass limits.)

We concentrate on the green (dark gray) region of Figure 7, where a relic density consistent with observations is obtained. Neutralino co-annihilation with the lightest stop is dominant where the stop-neutralino mass gap is small. As it is apparent from the figure, under the present missing-energy triggering requirements, the Tevatron will not be able to detect a light stop in this region of parameters.

Away from the region where co-annihilation becomes efficient, the top searches depend strongly on the masses of the neutralinos and charginos. As it is shown in the figure, prospects for stop detection improve dramatically so far the three body decay channel is suppressed by

$$m_{\tilde{t}} < m_{\chi^0} + m_W + m_b. \tag{6}$$

Searches at the Tevatron become more difficult for values of the stop and neutralino masses for which Eq. (6) is not fulfilled. For stop masses above 140 GeV, this always happens in the region of parameter space close to the one where the s-channel annihilation via the lightest CP-even Higgs becomes efficient, which is clearly seen as a narrow band around $m_{\tilde{Z}_1} \simeq 58$ GeV in Figure 7. In such a case, the three body decay mode becomes dominant, and the Tevatron, with less than 4 fb^{-1} integrated luminosity, cannot detect a light stop for any neutralino mass larger than 30 GeV [33].

Searches for the stop may be complemented by searches for charginos and neutralinos. An important channel is the trilepton one, that will allow to test these models for charginos masses up to about 130 GeV with 2 fb^{-1}. The value of the chargino mass in the gaugino region, $|\mu| \gtrsim 200$ GeV, may be approximately identified with the value of M_2, and using

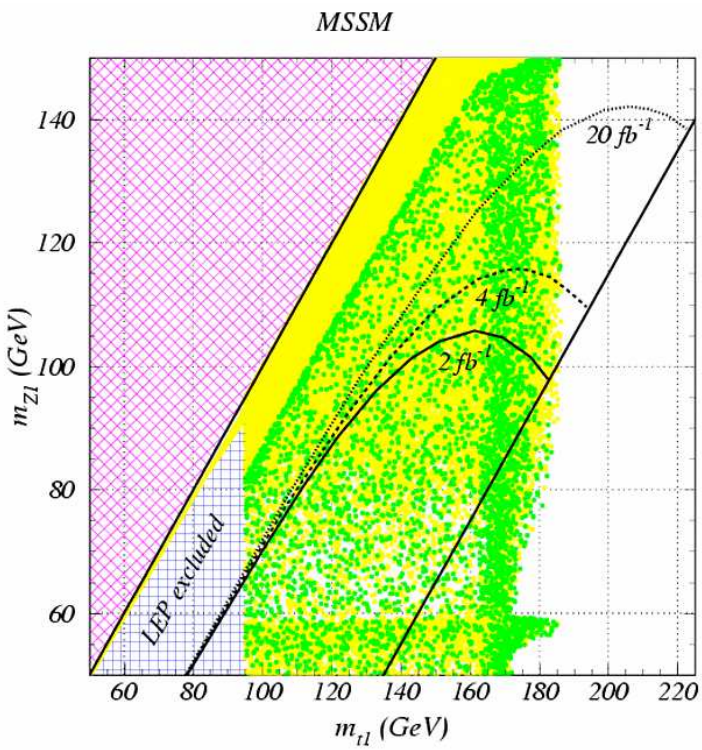

Figure 7: A random scan of parameter space projected on the stop mass vs. neutralino mass plane, as explained in the text in Eq. 5 and below. The dark-gray (green) region is the one in which the relic density is consistent with WMAP observations. In the light-gray (yellow) regions, the relic density is below the 2 σ WMAP bounds. The hatched regions are either excluded by LEP constraints (lower left) or inconsistent with the assumption of a neutralino LSP. Overlayed the Tevatron light stop search sensitivity in the $cc\not{E}_T$ channel for 2 (solid), 4 (dashed) and 20 (dotted) pb^{-1} integrated luminosity.

the standard relation between M_2 and M_1, $M_1 \simeq M_2/2$, this implies values of M_1 smaller than about 65 GeV [60, 61]. This covers the parameter space close to the region where s-channel annihilation via the lightest CP-even Higgs boson becomes relevant, in which stop searches become particularly difficult when the stop is heavier than 140 GeV.

Finally, we comment on future searches at the LHC. While the LHC will certainly be able to detect the charginos and neutralinos for all of the parameter space consistent with dark matter and a light stop, the search for a light stop may prove difficult in the co-annihilation region for similar reasons as at the Tevatron collider. Moreover, the dominant stop production and detection channels at the LHC come from the cascade decay of heavier colored particles and it will be difficult to disentangle the soft charm jets to identify the decaying top-squarks. A detailed study of LHC stop searches under these conditions is required to draw firm conclusions.

4 Direct dark matter detection

Missing energy signatures at hadron- and lepton-colliders provide very important evidence of the existence of a light, neutral, long-lived particle in the spectrum. Within supersymmetric models, this particle is identified with the LSP. But the stability of the lightest supersymmetric particle on the time scales required to contribute to the dark matter density cannot be checked by collider experiments. Direct detection of dark matter provides a complementary way of testing any particle physics explanation of the observed dark matter.

Neutralinos of astrophysical origin are searched for in neutralino-nucleon scattering experiments detecting elastic recoil of nuclei. The exclusion limits of these experiments are uniformly presented in the form of upper bounds on the (spin-independent) neutralino-proton scattering cross section (σ_{si}). It is also customary to scale the cross section by a factor of

$$f = \begin{cases} \Omega_{CDM}h^2/0.095 & \text{if } 0.095 \geq \Omega_{CDM}h^2, \\ 1 & \text{if } 0.095 < \Omega_{CDM}h^2 < 0.129, \end{cases} \tag{7}$$

to account for the diminishing flux of neutralinos with their decreasing density [62].

In Figure 8, we summarize the situation for dark matter detection in models with a stop lighter than the top quark, and the neutralino providing dark matter consistent with WMAP within 2 σ (green dots). Here we use the result of the random scan over the range of SUSY parameters defined by Eq. (5). For models marked by yellow (light gray) dots the neutralino relic density is below the 2 σ WMAP bound, while models represented by green (dark gray) dots comply with WMAP within 2 σ. The top solid (red) line represents the 2003 exclusion limit by Edelweiss [63], while the middle solid (magenta) line shows the 2004 exclusion limit by CDMS [64]. The lower lines indicate the projected sensitivity of the CDMS (solid blue) [65], ZEPLIN (dashed blue) [66] and XENON [67] (dotted blue) experiments. The 'hole' that appears at neutralino masses around 60-80 GeV and cross sections below 10^{-7} pb is due to the LEP stop-mass excluded region. This reflects the fact that small cross sections are induced only in the stop-neutralino co-annihilation region or in the resonant annihilation region via the light CP-even Higgs for large value of μ.

Prospects for direct detection of dark matter are quite good in most of the parameter space. Presently the region above the (red) top and (magenta) middle solid line is excluded by EDELWEISS and by CDMS, respectively. But the CDMS (solid blue) and ZEPLIN (dashed blue) experiments will probe large part of the relevant parameter space. Finally, XENON (dotted blue) will cover most of the interesting region.

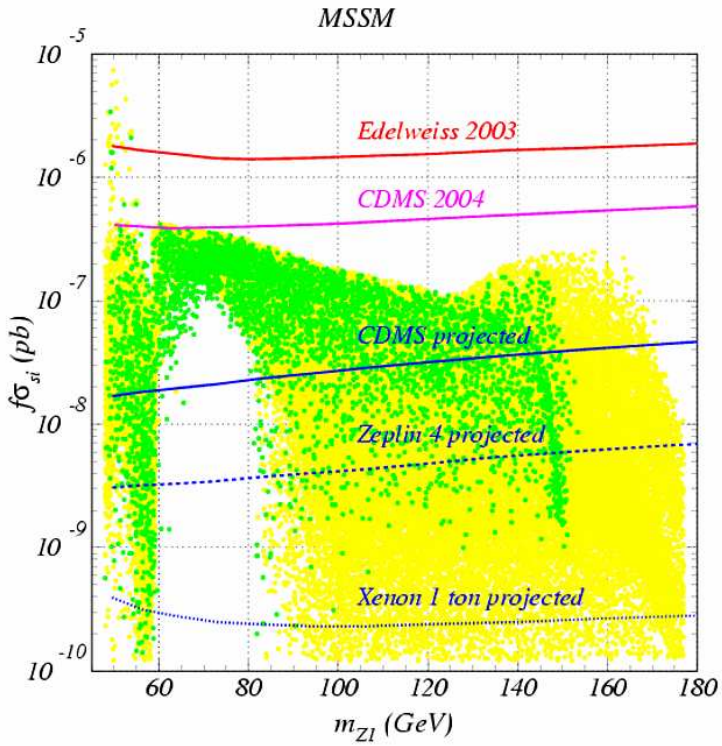

Figure 8: Spin independent neutralino-proton elastic scattering cross sections as a function of the neutralino mass. Green (dark gray) and yellow (light gray) dots represent models in which the neutralino density is consistent or below the 2 σ WMAP bounds. The top (red) and middle (magenta) solid lines represent the 2003 and 2004 exclusion limits by EDELWEISS and by CDMS, respectively. The lower solid, dashed, and dotted (blue) lines indicate the projected sensitivity of CDMS, ZEPLIN and XENON, respectively.

5 High-energy soft supersymmetry breaking parameters

The combined constraints of a light stop, as demanded for consistency with the electroweak baryogenesis scenario, and an acceptable dark matter relic density, imposes severe constraints on the soft supersymmetry breaking mass parameters of the theory. The stability of the lightest super-partner implies that the gravitino is heavier than the lightest neutralino and in turn supersymmetry must be broken at high energies, and transmitted to the observable sector at scales that are probably of order of the grand unification scale. It is interesting to know which boundary conditions of the mass parameters at high-energy scales could determine a low energy spectrum consistent with a light stop and a light neutralino.

Neutralino dark matter in the presence of a light stop has been studied in Ref. [68, 69] in the context of the minimal supergravity motivated model (mSUGRA). Electroweak

baryogenesis coupled with dark matter has also been examined in Ref. [70] within the same framework. It was found that for values of m_0, and $M_{1/2}$ of order of the weak scale and much larger values of A_0 ($|A_0| \gtrsim 1$ TeV) it is possible to obtain acceptable neutralino relic density in a narrow region of the parameter space consistent with electroweak baryogenesis. Presently, with considerably stronger Higgs mass limits and WMAP constraints on the cold dark matter, there is no mSUGRA parameter space where both dark matter and electroweak baryogenesis are satisfactory.

Based on these considerations, we shall work under the assumption that the gaugino masses unify at scales close to $M_{GUT} \simeq 10^{16}$ GeV, but we shall not assume unification of the scalar masses. Such boundary conditions are natural in models of superstrings, where the values of the supersymmetry breaking masses are determined by the vacuum expectation value of the auxiliary components of dilaton and moduli fields [71].

For large values of $\tan\beta$, the mass parameter associated with the Higgs acquiring the dominant vacuum expectation value is of the order of the weak scale,

$$m_2^2 \simeq -\frac{M_Z^2}{2}. \tag{8}$$

This mass parameter receives a supersymmetric contribution, proportional to the square of the μ parameter, as well as one coming from the supersymmetry breaking sector

$$m_2^2 = \mu^2 + m_{H_2}^2. \tag{9}$$

Eqs. (8) and (9) show that, in order to obtain values of $|\mu|$ of the order of the weak scale, $m_{H_2}^2$ must be negative, and of the order of the weak scale squared.

As discussed in Sec. 2, the realization of the mechanism of electroweak baryogenesis and the fulfillment of the present bounds on the lightest CP-even Higgs mass require right- and left-handed stop supersymmetry breaking parameters to be $m_{\tilde{U}_3} \simeq 0$ and $m_{\tilde{Q}_3} \gtrsim 1$ TeV, respectively. For values of $\tan\beta \lesssim 20$, for which the bottom-quark Yukawa effects may be neglected, the value of the low energy parameters are related to the values at high energies by the approximate relation [72]

$$\begin{aligned} m_{H_2}^2 &\simeq m_{H_2}^2(0) + 0.5 M_{1/2}^2 + \Delta m^2, \\ m_{\tilde{Q}_3}^2 &\simeq m_{\tilde{Q}_3}^2(0) + 7.1 M_{1/2}^2 + \frac{\Delta m^2}{3}, \\ m_{\tilde{U}_3}^2 &\simeq m_{\tilde{U}_3}^2(0) + 6.7 M_{1/2}^2 + \frac{2\,\Delta m^2}{3}, \end{aligned} \tag{10}$$

where $M_{1/2}$ is the common gaugino mass at scales of order of M_{GUT}, $m_i^2(0)$ denote the boundary condition of the scalar mass parameters at this scale, and Δm^2 represents the

negative radiative corrections governed by the large top-quark Yukawa coupling. Irrespectively of its form, the value of Δm^2 is related to $m^2_{\tilde{U}_3}(0)$ and $M^2_{1/2}$ by the relation

$$\begin{aligned}
\Delta m^2 &\simeq -\frac{3m^2_{\tilde{U}_3}(0)}{2} - 10M^2_{1/2} + \frac{3m^2_{\tilde{U}_3}}{2}, \\
m^2_{\tilde{Q}_3} &\simeq m^2_{\tilde{Q}_3}(0) - \frac{m^2_{\tilde{U}_3}(0)}{2} + 3.1M^2_{1/2} + \frac{m^2_{\tilde{U}_3}}{2}, \\
m^2_{H_2} &\simeq m^2_{H_2}(0) - \frac{3\, m^2_{\tilde{U}_3}(0)}{2} - 9.5M^2_{1/2} + \frac{3m^2_{\tilde{U}_3}}{2}.
\end{aligned} \tag{11}$$

Additional information comes from the form of Δm^2. The corrections depend on the square of the ratio of the Yukawa coupling to its quasi-fixed point value [72]. For values of $\tan\beta > 5$, this ratio is close to two thirds and one obtains, approximately

$$\Delta m^2 \simeq -\frac{m^2_{\tilde{Q}_3}(0) + m^2_{\tilde{U}_3}(0) + m^2_{H_2}(0)}{3} - \frac{A_0^2}{9} + 0.5A_0M_{1/2} - \frac{10}{3}M^2_{1/2}. \tag{12}$$

The value of $M_{1/2}$ is related to the value of M_1 by

$$M_1 \simeq 0.4M_{1/2}. \tag{13}$$

Therefore, the value of $M_{1/2}$ varies from values of about 400 GeV close to the stop-neutralino co-annihilation region, to values of about 150 GeV, close to the region where s-channel annihilation via the lightest CP-even Higgs boson becomes dominant. For these values of $\tan\beta$, and μ of the order of the weak scale, the low energy value of $X_t \simeq -A_t$, with

$$A_t = \frac{A_t(0)}{3} - 1.8M_{1/2}. \tag{14}$$

As discussed in Sec. 2, the acceptable values of the Higgs mass and of the phase transition strength are obtained for $0.3 \lesssim |X_t|/m_{\tilde{Q}_3} \lesssim 0.5$.

Finally, the square of the CP-odd Higgs mass m_A is approximately given by $m_1^2 + m_2^2$, or, approximately,

$$m_A^2 \simeq m^2_{H_1}(0) + 0.5M^2_{1/2} + \mu^2 - \frac{M_Z^2}{2}. \tag{15}$$

Solving for the high energy parameters, we obtain,

$$\begin{aligned}
m^2_{\tilde{U}_3}(0) &\simeq \frac{1}{3}\left(2m^2_{\tilde{Q}_3} - 2\mu^2 - M_Z^2 + 5m^2_{\tilde{U}_3} + 6A_t^2 + 32A_tM_1 - 160M_1^2\right), \\
m^2_{H_2}(0) &\simeq m^2_{\tilde{Q}_3} - 2\mu^2 - M_Z^2 + m^2_{\tilde{U}_3} + 3A_t^2 + 15A_tM_1 - 20M_1^2, \\
m^2_{\tilde{Q}_3}(0) &\simeq m^2_{\tilde{Q}_3} - 0.5m^2_{\tilde{U}_3} - 20M_1^2 + 0.5m^2_{\tilde{U}_3}(0), \\
A_t(0) &\simeq 3A_t + 13.5M_1.
\end{aligned} \tag{16}$$

Eqs. (15) and (16) determine the high-energy value of the soft supersymmetry breaking parameters in the Higgs and third generation squark sector. For positive boundary

conditions for the mass parameters, small values of m_A can only be obtained for very small or vanishing values of $m^2_{H_1}(0)$, and small values of $|\mu|$. Positive values of A_t tend to force all square mass parameters $m_i^2(0)$ to be large, of the order of 1–2 TeV squared, and the value of $A_t(0)$ becomes extremely large, of about 3 to 4 TeV.

For negative values of A_t, instead, the desired spectrum may be obtained for values of $m^2_{\tilde{U}_3}(0) \simeq 0$ and values of $A_t(0)$ smaller than about 1 TeV. The values of the other two square-mass parameters are of the same order, and of about a TeV-squared. Therefore, a more natural high-energy–low-energy connection is established for negative values of A_t. Using ISAJET 7.69 [50], we checked numerically that these conclusions remain valid even after the inclusion of higher loop RGE effects.

Finally, we mention that the main effect of increasing the value of $\tan\beta$ is to add negative corrections, induced by the bottom quark Yukawa coupling, to the parameters $m^2_{\tilde{Q}_3}$ and $m^2_{H_1}$ at low energies. Therefore, for larger values of $\tan\beta$, the required low energy spectrum would demand larger values of $m^2_{\tilde{Q}_3}(0)$ and $m^2_{H_1}(0)$. In particular, light CP-odd Higgs bosons become more natural for large values of $\tan\beta$.

6 Conclusions

The properties of the superpartners of the top quark have an important impact on the determination of the Higgs mass and also on the realization of the mechanism of electroweak baryogenesis in the MSSM. Light stops may arise due to the effect of mixing and also, as shown in section 5, due to large negative radiative corrections proportional to the square of the large top-quark Yukawa coupling.

In this article, we have studied the constraints that arise on supersymmetric models once the presence of a light stop and a consistent value of the dark matter relic density are required. We have shown that there are three different regions of parameter space in which these requirements may be fulfilled, associated with different neutralino annihilation channels. There are regions of parameter space where the s-channel annihilation into either Higgs bosons or Z-bosons become dominant, and appear for small values of M_1 and large or moderate values of $|\mu|$, respectively. The former regions depend strongly on the value of the CP-odd Higgs boson mass.

The presence of a light stop induces the existence of a third region, associated with co-annihilation between the stop and the lightest neutralino. In such region of parameters, unless the CP-odd Higgs boson is close to twice the neutralino mass, the stop-neutralino mass difference tends to be smaller than 30 GeV, presenting a serious challenge for stop searches at hadron colliders. The prospects for stop detection at the Tevatron collider

away from this region of parameters remain promising.

While the Tevatron will explore an important region of the MSSM parameter space compatible with electroweak baryogenesis and the observed dark matter density, the LHC will add in these searches by exploring the neutralino and chargino spectrum and complementing the existing Tevatron stop searches. The existence of the region where stop-neutralino co-annihilation becomes dominant motivates a dedicated analysis of stop searches at the LHC, in the regions where the stop-neutralino mass difference is small.

Under the standard assumptions of neutralino density and velocity distributions in our galaxy, prospects for direct dark-matter detection in the coming years are very promising in most of the MSSM parameter space of interest in this work. Direct dark matter searches present a complementary way of testing models of electroweak baryogenesis and dark matter, beyond the one provided by collider experiments.

Finally, we would like to emphasize that physics at a future linear collider [73] would be very important to test this scenario. On one hand, the LEP experience [28] shows that lepton colliders have the potential to detect a stop even in the cases of small mass differences between the stop and the lightest neutralino. On the other hand, a linear collider will provide the necessary precision to shed light on the nature and composition of both the light stop and the dark matter candidate.

Acknowledgements

Work at ANL is supported in part by the US DOE, Div. of HEP, Contract W-31-109-ENG-38. Fermilab is operated by Universities Research Association Inc. under contract no. DE-AC02-76CH02000 with the DOE. We thank G. Servant for invaluable discussions, and M. Schmitt and T. Tait for a critical reading of the manuscript.

References

[1] D. N. Spergel *et al.*, Astrophys. J. Suppl. **148**, 175 (2003) [arXiv:astro-ph/0302209].

[2] M. Tegmark *et al.* [SDSS Collaboration], arXiv:astro-ph/0310723.

[3] H. E. Haber and G. L. Kane, Phys. Rept. **117**, 75 (1985); H. P. Nilles, Phys. Rept. **110**, 1 (1984); S. P. Martin, arXiv:hep-ph/9709356.

[4] J. R. Ellis, K. A. Olive, Y. Santoso and V. C. Spanos, Phys. Lett. B **588**, 7 (2004) [arXiv:hep-ph/0312262].

[5] J. R. Ellis, K. A. Olive, Y. Santoso and V. C. Spanos, arXiv:hep-ph/0310356.

[6] R. Arnowitt, B. Dutta, B. Hu and Y. Santoso, Phys. Lett. B **505**, 177 (2001) [arXiv:hep-ph/0102344].

[7] J. L. Feng, S. Su and F. Takayama, arXiv:hep-ph/0404231.

[8] J. L. Feng, S. f. Su and F. Takayama, arXiv:hep-ph/0404198.

[9] A. Djouadi, M. Drees and J. L. Kneur, JHEP **0108**, 055 (2001) [arXiv:hep-ph/0107316].

[10] A. B. Lahanas, N. E. Mavromatos and D. V. Nanopoulos, Int. J. Mod. Phys. D **12**, 1529 (2003) [arXiv:hep-ph/0308251].

[11] A.D. Sakharov, *JETP Lett.* **91B** (1967) 24.

[12] M. Fukugita and T. Yanagida *Phys. Lett.* **B174** (1986) 45

[13] W. Buchmüller, P. Di Bari, M. Plümacher, *Nucl. Phys.* **B665** (2003) 445

[14] For reviews, see: A.G. Cohen, D.B. Kaplan and A.E. Nelson, *Ann. Rev. Nucl. Part. Sci.* **43** (1993) 27; M. Quirós, *Helv. Phys. Acta* **67** (1994) 451; V.A. Rubakov and M.E. Shaposhnikov, *Phys. Usp.* **39** (1996) 461; M. Carena and C.E.M. Wagner, hep-ph/9704347; A. Riotto, M. Trodden, *Ann. Rev. Nucl. Part. Sci.* **49** (1999) 35; M. Quirós and M. Seco, *Nucl. Phys.* **B Proc. Suppl. 81** (2000) 63, hep-ph/9703274.

[15] G. 't Hooft, Phys. Rev. D **14**, 3432 (1976) [Erratum-ibid. D **18**, 2199 (1978)];

[16] A. G. Cohen, D. B. Kaplan and A. E. Nelson, *Phys. Lett.* **B336** (1994) 41 [arXiv:hep-ph/9406345].

[17] N.S. Manton, *Phys. Rev.* **D28** (1983) 2019; F.R. Klinkhamer and N.S. Manton, *Phys. Rev.* **D30** (1984) 2212.

[18] D. Bodeker, *Phys. Lett.* **B426** (1998) 351 [arXiv:hep-ph/9801430]; P. Arnold and L.G. Yaffe, hep-ph/9912306; P. Arnold, *Phys. Rev.* **D62** (2000) 036003; G.D. Moore and K. Rummukainen, *Phys. Rev.* **D61** (2000) 105008; G.D. Moore, *Phys. Rev.* **D62** (2000) 085011.

[19] K. Jansen, *Nucl. Phys.* **B Proc. Suppl. 47** (1996) 196, hep-lat/9509018; K. Rummukainen, M. Tsypin, K. Kajantie, M. Laine and M. Shaposhnikov, *Nucl. Phys.* **B532** (1998) 283; K. Rummukainen, K. Kajantie, M. Laine, M. Shaposhnikov and M. Tsypin, hep-ph/9809435.

[20] M. Carena, M. Quirós and C.E.M. Wagner, *Phys. Lett.* **B380** (1996) 81.

[21] M. Laine, *Nucl. Phys.* **B481** (1996) 43; M. Losada, *Phys. Rev.* **D56** (1997) 2893; G. Farrar and M. Losada, *Phys. Lett.* **B406** (1997) 60.

[22] B. de Carlos and J.R. Espinosa, *Nucl. Phys.* **B503** (1997) 24.

[23] D. Bodeker, P. John, M. Laine and M.G. Schmidt, *Nucl. Phys.* **B497** (1997) 387.

[24] M. Carena, M. Quirós and C.E.M. Wagner, *Nucl. Phys.* **B524** (1998) 3.

[25] M. Laine, K. Rummukainen, *Nucl. Phys.* **B535** (1998) 423.

[26] M. Losada, *Nucl. Phys.* **B537** (1999) 3 and *Nucl. Phys.* **B569** (2000) 125; M. Laine and M. Losada, *Nucl. Phys.* **B582** (2000) 277.

[27] M. Laine and K. Rummukainen, *Nucl. Phys.* **B597** (2001) 23 [arXiv:hep-lat/0009025].

[28] LEP2 SUSY Working Group *Combined LEP stop and sbottom results 183-208 GeV*, `http://lepsusy.web.cern.ch/lepsusy/www/squarks_summer02/squarks_pub.html`.

[29] T. Affolder *et al.* [CDF Collaboration], Phys. Rev. Lett. **84**, 5704 (2000) [arXiv:hep-ex/9910049]; S. Abachi *et al.* [D0 Collaboration], Phys. Rev. Lett. **76**, 2222 (1996).

[30] M. Carena, D. Choudhury, R. A. Diaz, H. E. Logan and C. E. M. Wagner, Phys. Rev. D **66**, 115010 (2002) [arXiv:hep-ph/0206167].

[31] E. L. Berger, B. W. Harris and Z. Sullivan, Phys. Rev. Lett. **83**, 4472 (1999) [arXiv:hep-ph/9903549]; E. L. Berger, B. W. Harris and Z. Sullivan, Phys. Rev. D **63**, 115001 (2001) [arXiv:hep-ph/0012184].

[32] C. L. Chou and M. E. Peskin, Phys. Rev. D **61**, 055004 (2000) [arXiv:hep-ph/9909536].

[33] R. Demina, J. D. Lykken, K. T. Matchev and A. Nomerotski, Phys. Rev. D **62**, 035011 (2000);

[34] S. Heinemeyer, W. Hollik, and G. Weiglein, Phys. Rev. D **58**, 091701 (1998) [arXiv:hep-ph/9803277]; S. Heinemeyer, W. Hollik, and G. Weiglein, Phys. Lett. B **440**, 296 (1998) [arXiv:hep-ph/9807423]; S. Heinemeyer, W. Hollik, and G. Weiglein, wo-loop level," Eur. Phys. J. C **9**, 343 (1999) [arXiv:hep-ph/9812472];

M. Carena, M. Quiros, and C. E. M. Wagner, Nucl. Phys. B **461**, 407 (1996) [arXiv:hep-ph/9508343]; H. E. Haber, R. Hempfling, and A. H. Hoang, Z. Phys. C **75**, 539 (1997) [arXiv:hep-ph/9609331]; J. R. Espinosa and R. J. Zhang, J. High Energy Phys. **0003**, 026 (2000) [arXiv:hep-ph/9912236]; J. R. Espinosa and R. J. Zhang, Nucl. Phys. B **586**, 3 (2000) [arXiv:hep-ph/0003246]; M. Carena, H. E. Haber, S. Heinemeyer, W. Hollik, C. E. M. Wagner, and G. Weiglein, Nucl. Phys. B **580**, 29 (2000) [arXiv:hep-ph/0001002]; G. Degrassi, P. Slavich, and F. Zwirner, Nucl. Phys. B **611**, 403 (2001) [arXiv:hep-ph/0105096]; A. Brignole, G. Degrassi, P. Slavich, and F. Zwirner, arXiv:hep-ph/0112177; S. P. Martin, Phys. Rev. D **67**, 095012 (2003) [arXiv:hep-ph/0211366].

[35] R. Barate *et al.* [ALEPH Collaboration], Phys. Lett. B **565**, 61 (2003) [arXiv:hep-ex/0306033].

[36] J. M. Cline, M. Joyce and K. Kainulainen, JHEP **0007**, 018 (2000) [arXiv:hep-ph/0006119]; M. Carena, J. M. Moreno, M. Quiros, M. Seco and C. E. Wagner, *Nucl. Phys.* **B599** (2001) 158; M. Carena, M. Quiros, M. Seco and C. E. M. Wagner, Nucl. Phys. B **650**, 24 (2003) [arXiv:hep-ph/0208043].

[37] M. E. Gomez, T. Ibrahim, P. Nath and S. Skadhauge, arXiv:hep-ph/0404025.

[38] T. Nihei and M. Sasagawa, the arXiv:hep-ph/0404100.

[39] M. Argyrou, A. B. Lahanas, D. V. Nanopoulos and V. C. Spanos, CP - arXiv:hep-ph/0404286.

[40] See, for example, J. S. Lee, A. Pilaftsis, M. Carena, S. Y. Choi, M. Drees, J. R. Ellis and C. E. M. Wagner, Comput. Phys. Commun. **156**, 283 (2004) [arXiv:hep-ph/0307377]; M. Carena, J. R. Ellis, A. Pilaftsis and C. E. M. Wagner, Nucl. Phys. B **625**, 345 (2002) [arXiv:hep-ph/0111245]; T. Ibrahim and P. Nath, Phys. Rev. D **66**, 015005 (2002) [arXiv:hep-ph/0204092]; S. Heinemeyer, Eur. Phys. J. C **22**, 521 (2001) [arXiv:hep-ph/0108059]; S. Y. Choi, M. Drees and J. S. Lee, Phys. Lett. B **481**, 57 (2000) [arXiv:hep-ph/0002287].

[41] C. Balázs, M. Carena, D. Morrissey, A. Menon and C.E.M. Wagner, work in progress.

[42] G. W. Bennett *et al.* [Muon g-2 Collaboration], Phys. Rev. Lett. **89**, 101804 (2002) [Erratum-ibid. **89**, 129903 (2002)] [arXiv:hep-ex/0208001].

[43] J. F. de Troconiz and F. J. Yndurain, arXiv:hep-ph/0402285.

[44] T. Kinoshita and M. Nio, arXiv:hep-ph/0402206.

[45] S. Heinemeyer, D. Stockinger and G. Weiglein, arXiv:hep-ph/0312264.

[46] K. Hagiwara, A. D. Martin, D. Nomura and T. Teubner, arXiv:hep-ph/0312250.

[47] K. Melnikov and A. Vainshtein, arXiv:hep-ph/0312226.

[48] M. Davier, S. Eidelman, A. Hocker and Z. Zhang, Eur. Phys. J. C **31**, 503 (2003) [arXiv:hep-ph/0308213].

[49] H. Baer, C. Balázs, J. Ferrandis and X. Tata, Phys. Rev. D **64**, 035004 (2001) [arXiv:hep-ph/0103280].

[50] F. E. Paige, S. D. Protopescu, H. Baer and X. Tata, arXiv:hep-ph/0312045.

[51] H. Baer, C. Balázs and A. Belyaev, JHEP **0203**, 042 (2002) [arXiv:hep-ph/0202076].

[52] G. Belanger, F. Boudjema, A. Pukhov and A. Semenov, Comput. Phys. Commun. **149**, 103 (2002) [arXiv:hep-ph/0112278].

[53] H. Baer, C. Balázs, A. Belyaev and J. O'Farrill, JCAP **0309**, 007 (2003) [arXiv:hep-ph/0305191].

[54] LEP2 SUSY Working Group *Combined LEP Chargino Results, up to 208 GeV*, `http://lepsusy.web.cern.ch/lepsusy/www/inos_moriond01/charginos_pub.html`.

[55] H. V. Klapdor-Kleingrothaus, Nucl. Phys. Proc. Suppl. **110**, 364 (2002) [arXiv:hep-ph/0206249]. D. B. Cline, H. g. Wang and Y. Seo, in *Proc. of the APS/DPF/DPB Summer Study on the Future of Particle Physics (Snowmass 2001)* ed. N. Graf, eConf **C010630**, E108 (2001) [arXiv:astro-ph/0108147].

[56] D. Abrams *et al.* [CDMS Collaboration], Phys. Rev. D **66**, 122003 (2002) [arXiv:astro-ph/0203500]; A. Benoit *et al.*, Phys. Lett. B **545**, 43 (2002) [arXiv:astro-ph/0206271]; D. Cline *et al.*, *Prepared for 3rd International Conference on Dark Matter in Astro and Particle Physics (Dark 2000), Heidelberg, Germany, 10-16 Jul 2000*

[57] M. Ciuchini, G. Degrassi, P. Gambino and G. F. Giudice, Nucl. Phys. B **534**, 3 (1998) [arXiv:hep-ph/9806308]. G. Degrassi, P. Gambino and G. F. Giudice, JHEP **0012**, 009 (2000) [arXiv:hep-ph/0009337]. M. Carena, D. Garcia, U. Nierste and C. E. M. Wagner, Phys. Lett. B **499**, 141 (2001) [arXiv:hep-ph/0010003].

[58] F. Gabbiani, E. Gabrielli, A. Masiero and L. Silvestrini, Nucl. Phys. B **477**, 321 (1996) [arXiv:hep-ph/9604387].

[59] M. Carena, S. Mrenna and C. E. M. Wagner, Phys. Rev. D **60**, 075010 (1999) [arXiv:hep-ph/9808312].

[60] K. T. Matchev and D. M. Pierce, Phys. Rev. D **60**, 075004 (1999).

[61] S. Abel *et al.* [SUGRA Working Group Collaboration], arXiv:hep-ph/0003154.

[62] J. R. Ellis, A. Ferstl and K. A. Olive, Phys. Rev. D **63**, 065016 (2001) [arXiv:hep-ph/0007113].

[63] G. Chardin *et al.* [EDELWEISS Collaboration], DAPNIA-03-276 *Prepared for 4th International Conference on Physics Beyond the Standard Model: Beyond the Desert (BEYOND 03), Castle Ringberg, Tegernsee, Germany, 9-14 Jun 2003*

[64]

[64] D. S. Akerib *et al.* [CDMS Collaboration], arXiv:astro-ph/0405033;

[65] L. Baudis [CDMS Collaboration], eConf **C020805**, TF02 (2002).

[66] D. B. Cline *et al.*, Nucl. Phys. Proc. Suppl. **124**, 229 (2003).

[67] E. Aprile, talk given at the 6th UCLA Symposium on Sources and Detection of Dark Matter and Dark Energy in the Universe, February 18-20, 2004 at the Marina Beach Marriott, Marina del Rey, California (http://www.physics.ucla.edu/hep/dm04/talks/aprile.pdf)

[68] C. Boehm, A. Djouadi and M. Drees, Phys. Rev. D **62**, 035012 (2000) [arXiv:hep-ph/9911496].

[69] J. R. Ellis, K. A. Olive and Y. Santoso, Astropart. Phys. **18**, 395 (2003) [arXiv:hep-ph/0112113].

[70] S. Davidson, T. Falk and M. Losada, Phys. Lett. B **463**, 214 (1999)

[71] A. Brignole, L. E. Ibanez and C. Munoz, Nucl. Phys. B **422**, 125 (1994) [Erratum-ibid. B **436**, 747 (1995)] [arXiv:hep-ph/9308271].

[72] M. Carena, M. Olechowski, S. Pokorski and C. E. M. Wagner, Nucl. Phys. B **419**, 213 (1994)

[73] T. Abe *et al.* [American Linear Collider Working Group Collaboration], in *Proc. of the APS/DPF/DPB Summer Study on the Future of Particle Physics (Snowmass 2001)* ed. N. Graf, arXiv:hep-ex/0106056; J. A. Aguilar-Saavedra *et al.* [ECFA/DESY LC Physics Working Group Collaboration], arXiv:hep-ph/0106315.